# Disturbance Compensator for a Very Flexible Parallel Lambda Robot in Trajectory Tracking

Fatemeh Ansarieshlaghi[a] and Peter Eberhard[b]
*Institute of Engineering and Computational Mechanics, University of Stuttgart, Pfaffenwaldring 9, 70569 Stuttgart, Germany*

Keywords: Flexible Parallel Robot, Position Control, Disturbance Observer, Disturbance Compensator.

Abstract: This research investigates the design of a nonlinear position controller and a disturbance observer to estimate and compensate disturbances on a very flexible parallel robot to improve trajectory tracking and control performance. The used robot has very flexible links and can be considered as an underactuated system since it has fewer control inputs than degrees of freedom for rigid body motions and deformations. Hence, these flexibilities must be taken into account in the control design. To obtain high performance in the end-effector trajectory tracking, an accurate and efficient nonlinear controller is required. This nonlinear controller includes a position controller and a disturbance observer. The nonlinear feedback controller is designed based on the feedback linearization approach and its stability is proofed by the Lyapunov candidate function. The disturbances that are investigated in this work are the friction forces of the drives of the robot, acting forces on the robot's end-effector, and their combination. The designed nonlinear controller is implemented on the simulated model of the robot under different disturbances. The simulation results show that the end-effector tracks desired trajectories with higher accuracy and better performance in comparison to other controllers in previous works. Also, by the designed nonlinear position controller and the disturbance observer the robot tracks the desired trajectory with the highest robustness under disturbances in comparison to the previous work.



## 1 INTRODUCTION

Robot manipulators attract a lot of research interest because of their applications. The applications of the manipulators are industrial, surgical, soft robotics, etc. Based on the robot body design, the manipulators can be divided into rigid designs and light-weight designs. In the rigid designs, the manipulator and its links are usually built based on the maximum stiffness to avoid oscillation and deformation. This design needs a lot of material and strong power supplies. In contrast, the light-weight design minimizes material, energy usage, and yields often high working speeds. However, due to the light-weight design, the bodies have significant flexibility which yields undesired deformations and vibrations. Therefore, these manipulators are modeled as a flexible multibody system and the flexibilities must be taken into account in the control design. The flexible system with significant deformations complicates the control design because there are more generalized coordinates than control inputs. In order to obtain a high performance in the end-effector trajectory tracking of a flexible manipulator, an accurate and efficient model and a nonlinear controller are necessary. The difficulty and complexity of designing a nonlinear feedback controller with high performance for a highly flexible system are increased when the system is under unknown disturbances. To overcome this problem, an observer to estimate system disturbances is required. Finally, based on the estimated disturbances on the system by the designed disturbance observer one can compensate disturbances on the system during trajectory tracking by a nonlinear position controller.

The used manipulator in this paper is a parallel robot manipulator. This robot has highly flexible links. The end of the short link is connected in the middle of the long link and described using rigid bodies. The links connection creates a $\lambda$-shape configuration and a closed-loop kinematics constraint result that presents the parallel configuration of the robot.

In previous works on the lambda robot, the nonlinear feedback controllers just investigate trajectory tracking tasks, see (Ansarieshlaghi and Eberhard,

[a] https://orcid.org/0000-0003-2693-0882
[b] https://orcid.org/0000-0003-1809-4407



Ansarieshlaghi, F. and Eberhard, P.
Disturbance Compensator for a Very Flexible Parallel Lambda Robot in Trajectory Tracking.
DOI: 10.5220/0009790203940401
In *Proceedings of the 17th International Conference on Informatics in Control, Automation and Robotics (ICINCO 2020)*, pages 394-401
ISBN: 978-989-758-442-8

2018b; Eberhard and Ansarieshlaghi, 2019) without investigation of the controller's robustness on the distributed system.

The novelty of this work is, that a nonlinear feedback controller for high-speed trajectory tracking of a very flexible parallel lambda robot is designed based on the feedback linearization approach and this controller consists of a position controller and a disturbance observer. The disturbance observer estimates disturbances and the position controller computes the controller input for tracking a desired trajectory by the robot.

The disturbances on systems can be divided into two groups, see (Chen et al., 2016), i.e., the first group is included the disturbances that are known and measurable and they can be compensated by the computed feedforward input controller, the second group is disturbances which are not measurable or measuring them are very expensive. Furthermore, the second group of disturbances needs to estimate and compensate for their influences on systems. The disturbance observer has wide application in mechatronics systems, see (Han, 2009; Chen et al., 2016; Mohammadi et al., 2017; Liu et al., 2018), these systems needs for high precision and high performance during doing the desired tasks while there are disturbances affected to the systems. These disturbances can be caused by external disturbances, such as torques, forces during invasive surgery (Mohammadi et al., 2017), vibrations of horizontal position of a rail track, and frictions of the prismatic joints (Morlock et al., 2015) or subjected of internal model parameter as the changes of operating conditions or external working environments and model simplification (Chen et al., 2000; Chen, 2004). These described disturbances, external and internal disturbances can be formulated as a variable and then by disturbance observer is tried to estimate and compensate them.

The disturbance observer estimates the disturbances that are applied to the joints and the end-effector and then, it adapts the controlled robot to the operating environmental conditions. The nonlinear feedback controller consisting of the nonlinear disturbance observer and position controller which they compute the robot inputs. The designed feedback controller is simulated on the lambda robot model. Simulation results of the designed controller on the lambda robot show that the end-effector tracks a trajectory with high accuracy and the tracking performance of the system under disturbances is drastically improved compared to previous work (Ansarieshlaghi and Eberhard, 2018b). Also, the simulation results show that the robustness performance of the feedback controller is increased by the designed disturbance observer.

This paper is organized as follows: Section 2 describes the lambda robot, its components, and its hardware setup. Section 3 consists of the modeling of the flexible parallel lambda robot. Section 4 includes the description of the nonlinear control, i.e., the feedforward controller, position controller, and nonlinear disturbance observer. In Section 5, the proposed nonlinear controller is implemented on the simulated model and the results are discussed. Finally, the conclusions of the paper are presented in Section 6.

## 2 FLEXIBLE LAMBDA ROBOT

The lambda robot has its name coming from its physical appearance which looks like the Greek letter λ shown in Figure 1. This robot consists of two links, three revolute joints, and two prismatic joints. With one of the links being shorter, roughly half the size of the other, the characteristic appearance of the lambda robot is created. The prismatic joints are realized with two direct drives, each moving along their linear axis parallel to each other. Both drives are controlled by a servomotor. On each prismatic joint, one passive revolute joint is fixed, providing a connection to the links. The third revolute joint connects the end of the short link to the middle of the long one. The long link also has an additional mass installed at its end, which represents an end-effector.

The robot end-effector can only move in a two-dimensional plane, making the system planar. The link design is very flexible. Furthermore, the robot is characterized as a flexible planar parallel manipulator.

The drive positions and velocities of the robot are measured with two optical encoders. Two full Wheatstone bridge strain gauge sets are attached to the long flexible link to measure its deformation. The lambda robot configuration is shown in Figure 1 has been built in hardware, see (Burkhardt et al., 2014) at the Institute of Engineering and Computational Mechanics of the University of Stuttgart.

## 3 MODELING OF THE FLEXIBLE LAMBDA ROBOT

The modeling process of the flexible manipulator with λ configuration is divided into three major steps. In the first step, the flexible components of the robot links are modeled with the linear finite element method in the commercial finite element code *ANSYS* with six hundred degrees of freedom in total. Next,

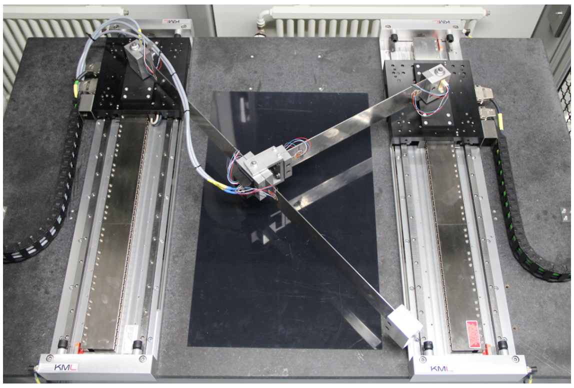

Figure 1: Lambda robot.

for controlling the $\lambda$ robot, the degrees of freedom of the flexible bodies are decreased. Therefore, the modal model order reduction method is utilized to reduce the order of the flexible multibody model. Finally, all the rigid and flexible parts are modeled as a multibody system with a kinematic loop. The equation of motion with a kinematic loop constraint of the flexible parallel manipulator using the generalized coordinates $\boldsymbol{q} \in \boldsymbol{R}^5$ is formulated as

$$\boldsymbol{M}(\boldsymbol{q})\ddot{\boldsymbol{q}} = \boldsymbol{f}'(\boldsymbol{q},\dot{\boldsymbol{q}}) + \boldsymbol{B}(\boldsymbol{q})\boldsymbol{u} + \boldsymbol{C}^{\mathrm{T}}(\boldsymbol{q})\boldsymbol{\lambda}. \quad (1)$$

The symmetric, positive definite mass matrix $\boldsymbol{M} \in \boldsymbol{R}^{5\times5}$ depends on the joint angles and the elastic coordinates. The vector $\boldsymbol{f}'(\boldsymbol{q},\dot{\boldsymbol{q}}) = \boldsymbol{g}(\boldsymbol{q},\dot{\boldsymbol{q}}) - \boldsymbol{k}(\boldsymbol{q},\dot{\boldsymbol{q}})$ contains $\boldsymbol{k} \in \boldsymbol{R}^5$, the vector of the generalized centrifugal, Coriolis and Euler forces, and $\boldsymbol{g} \in \boldsymbol{R}^5$ includes the vector of applied forces and inner forces due to the body elasticity. The input matrix $\boldsymbol{B} \in \boldsymbol{R}^{5\times2}$ maps the input vector $\boldsymbol{u} \in \boldsymbol{R}^2$ to the system in Equation 1. The constraint equations are defined by $\boldsymbol{c} \in \boldsymbol{R}^2$ as

$$\boldsymbol{c}(\boldsymbol{q}) = \boldsymbol{0}. \quad (2)$$

The Jacobian matrix of the constraint $\boldsymbol{C} = \partial(\boldsymbol{c}(\boldsymbol{q}))/\partial\boldsymbol{q} \in \boldsymbol{R}^{2\times5}$ maps the reaction force $\boldsymbol{\lambda} \in \boldsymbol{R}^2$ due to the kinematic loop. The flexible lambda robot model is shown in Figure 2, see also (Burkhardt et al., 2014; Ansarieshlaghi and Eberhard, 2018a; Ansarieshlaghi and Eberhard, 2018b).

The lambda robot's generalized coordinates are defined by $\boldsymbol{q} = [s_1, s_2, \alpha_1, \alpha_2, q_e]^T$. The driver positions are described by $s_1$ and $s_2$ as shown in Figure 2. The angle between the long link and the movement direction of the long link prismatic joint is $\alpha_1$ and $\alpha_2$ is defined as shown in Figure 2. The long link is modeled as flexible and its flexible generalized coordinate is described by $q_e$.

The vector $\boldsymbol{\lambda} = \boldsymbol{n}(\boldsymbol{q},\dot{\boldsymbol{q}},\boldsymbol{u})$ is a function of the system states $(\boldsymbol{q},\dot{\boldsymbol{q}})$ and the system input $\boldsymbol{u}$. To simply the system dynamics, this vector can be written as

$$\boldsymbol{\lambda} = \boldsymbol{\lambda}_{\mathrm{q}} + \boldsymbol{\lambda}_{\mathrm{u}}\boldsymbol{u}, \quad (3)$$

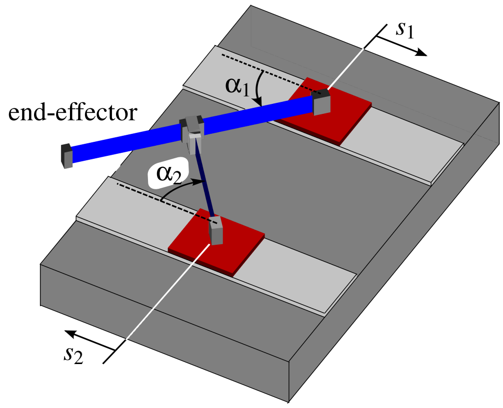


Figure 2: Simulation model of the very flexible parallel lambda robot.

where $\boldsymbol{\lambda}_{\mathrm{q}}$ is vector of the system states $(\boldsymbol{q},\dot{\boldsymbol{q}})$ and $\boldsymbol{\lambda}_{\mathrm{u}}$ is a function of the system inputs $(\boldsymbol{u})$. Hence, the system dynamics formulation in Equation (1) is reformulated

$$\boldsymbol{M}(\boldsymbol{q})\ddot{\boldsymbol{q}} = \boldsymbol{f}(\boldsymbol{q},\dot{\boldsymbol{q}}) + \boldsymbol{B}_{\mathrm{u}}(\boldsymbol{q})\boldsymbol{u}, \quad (4)$$

where vector $\boldsymbol{f}$ is calculated by $\boldsymbol{f} = \boldsymbol{f}' + \boldsymbol{C}^T\boldsymbol{\lambda}_{\mathrm{q}}$ and matrix $\boldsymbol{B}_{\mathrm{u}}$ is formulated as $\boldsymbol{B}_{\mathrm{u}} = \boldsymbol{B} + \boldsymbol{C}^T\boldsymbol{\lambda}_{\mathrm{u}}$.

## 4 CONTROL OF THE FLEXIBLE LAMBDA ROBOT

The lambda robot controller design is separated into feedforward and feedback controller parts. In the feedforward part, the desired signals are calculated based on the robot workspace, the joint space, the kinematics, and the dynamics constraints of the robot. The kinematics constraints include the maximum velocity, position of the robot joints, and the closed-loop kinematics. The maximum current and the maximum flexible coordinates oscillation amplitude are defined as dynamics constraints, see (Seifried et al., 2011). The feedback control part computes the lambda robot inputs based on the feedback linearization approch (Khalil, 2002) using the nonlinear dynamics of the robot and the system states.

The feedforward part computes desired signals for the system generalized coordinate as $\boldsymbol{q}_{\mathrm{d}}$, their derivative $\dot{\boldsymbol{q}}_{\mathrm{d}}$, and feedforward input $\boldsymbol{u}_{\mathrm{ff}}$ based on the desired end-effector trajectory. In the feedback controller, the input $\boldsymbol{u}$ is calculated based on the desired variables which are fed to the feedback controller and measured or observed variables as $\boldsymbol{q}$ and $\dot{\boldsymbol{q}}$ which are shown in Figure 3.

The nonlinear feedback controller for the position controller of the lambda robot is divided into the joint space controller and the Cartesian space controller.

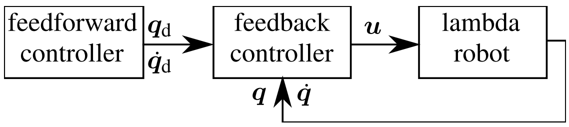


Figure 3: Nonlinear control structure.

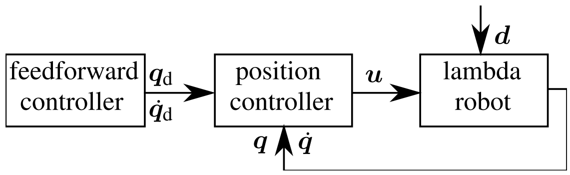


Figure 4: Nonlinear position control structure under disturbances.

In the position controller in the joint space, the controller includes a position controller, see (Eberhard and Ansarieshlaghi, 2019) and alternatively a position controller and a state observer, see (Ansarieshlaghi and Eberhard, 2018b). Also, for controlling the end-effector position in the workspace, a position controller and its combination with the forward kinematics are designed and implemented on the simulated model of the robot (Ansarieshlaghi and Eberhard, 2019). In contrast to the previous works, the robot is here disturbed by forces that are acting to the robot joint space and workspace shown in Figure 4.

To do the desired, trajectory tracking, a model-based controller is required to guarantee the robot performance. Hence, the Lyapunov method (Khalil, 2002) is used to prove the stability of the controlled system. This nonlinear controller is not able to adapt to unknown influences of disturbances. Hence, to increase tracking performance and controller robustness, the feedback controller is developed for the system under disturbances by adding a part to obtain disturbances. These disturbances are estimated by the disturbance observer approach which is presented in (Chen et al., 2016; Mohammadi et al., 2017).

In this work, the feedback controller is divided into the position controller and the disturbance observer. In the first part, the position controller design for the system is presented in Section 4.1 and its stability by the designed controller is investigated by the Lyapunov function. Then, for the system under disturbances, the Lyapunov function stability is developed and these disturbances are estimated with the disturbance observer in Section 4.2.

## 4.1 Position Controller

To design a nonlinear feedback controller for the system in Equation (4), the control law is obtained for the lambda robot as

$$\boldsymbol{u} = \boldsymbol{B}_{\mathrm{u}}^{-1}(-\boldsymbol{f} + \boldsymbol{M}(\boldsymbol{K}_{\mathrm{P}}\boldsymbol{e} + \boldsymbol{K}_{\mathrm{D}}\dot{\boldsymbol{e}})), \quad (5)$$

where the error and its dynamics are computed by $\boldsymbol{e} = \boldsymbol{q} - \boldsymbol{q}_{\mathrm{d}}$ and $\dot{\boldsymbol{e}} = \dot{\boldsymbol{q}} - \dot{\boldsymbol{q}}_{\mathrm{d}}$. The vector $\boldsymbol{q}_{\mathrm{d}}$ is the desired value for $\boldsymbol{q}$ and $\dot{\boldsymbol{q}}_{\mathrm{d}}$ is the desired value for $\dot{\boldsymbol{q}}$. The desired values depend on the desired trajectory of the end-effector and can be computed via the feedforward part and $\boldsymbol{q}_{\mathrm{d}}$ and $\dot{\boldsymbol{q}}_{\mathrm{d}}$ can be set. The matrices $\boldsymbol{K}_{\mathrm{P}}$ and $\boldsymbol{K}_{\mathrm{D}}$ correspond to the weighting of feedback errors and can be designed via the LQR method or tuned by hand. Also, they should satisfy the stability conditions for non-autonomous systems for uniform stability, based on the Lyapunov theorem. The inverse of the input matrix $\boldsymbol{B}_{\mathrm{u}}$ is not straightforward to calculate, since it is not of full row rank. Therefore, the existing left-inverse is used as a pseudo-inverse to yield $\boldsymbol{B}_{\mathrm{u}}^{-1}\boldsymbol{B}_{\mathrm{u}} = \boldsymbol{I}$. The vector $\boldsymbol{u}$ presents the control input of the robot manipulator and is the output of the designed position controller.

Here, the desired trajectory given by $\boldsymbol{q}_{\mathrm{d}}$, $\dot{\boldsymbol{q}}_{\mathrm{d}}$ are time-variant and therefore, the system is non-autonomous. Also, the system is underactuated and the underactuated joints $\boldsymbol{q}_u = [\alpha_1, \alpha_2, q_{\mathrm{e}}]$ are function of the actuated joints $\boldsymbol{q}_a = [s_1, s_2]^T$ which are described by the system dynamics. Therefore, the Lyapunov candidate function is defined for the actuated joints as

$$V(\boldsymbol{e}_{\mathrm{a}}, \dot{\boldsymbol{e}}_{\mathrm{a}}) = \dot{\boldsymbol{e}}_{\mathrm{a}}^T \boldsymbol{P}\, \dot{\boldsymbol{e}}_{\mathrm{a}} + \boldsymbol{e}_{\mathrm{a}}^T \boldsymbol{A}\, \boldsymbol{e}_{\mathrm{a}}, \quad (6)$$

where the matrices $\boldsymbol{P} \in \boldsymbol{R}^{2\times 2}$ and $\boldsymbol{A} \in \boldsymbol{R}^{2\times 2}$ are positive-definite matrices and the active joints tracking errors and their dynamics are presented by $\boldsymbol{e}_{\mathrm{a}}$ and $\dot{\boldsymbol{e}}_{\mathrm{a}}$, respectively. To proof stability by the designed controller, the Lyapunov function and its derivative must be continuous and fulfill the conditions

$$\beta(\|[\boldsymbol{e}_{\mathrm{a}}, \dot{\boldsymbol{e}}_{\mathrm{a}}]^T\| \geq V(\boldsymbol{e}_{\mathrm{a}}, \dot{\boldsymbol{e}}_{\mathrm{a}}) \geq \alpha(\|[\boldsymbol{e}_{\mathrm{a}}, \dot{\boldsymbol{e}}_{\mathrm{a}}]^T\|). \quad (7)$$

The functions $\alpha$ and $\beta$ are class $\mathcal{K}$. Therefore, the Lyapunov candidate function $\alpha = \beta = V$ is class $\mathcal{K}$, too. This definition of class $\mathcal{K}$ can be found in (Khalil, 2002). The derivative of the Lyapunov candidate function is computed as

$$\begin{aligned} \dot{V} &= \ddot{\boldsymbol{e}}_{\mathrm{a}}^T \boldsymbol{P}\, \dot{\boldsymbol{e}}_{\mathrm{a}} + \dot{\boldsymbol{e}}_{\mathrm{a}}^T \boldsymbol{P}\, \ddot{\boldsymbol{e}}_{\mathrm{a}} + \dot{\boldsymbol{e}}_{\mathrm{a}}^T \boldsymbol{A}\, \boldsymbol{e}_{\mathrm{a}} + \boldsymbol{e}_{\mathrm{a}}^T \boldsymbol{A}\, \dot{\boldsymbol{e}}_{\mathrm{a}} \\ &= \left(\boldsymbol{M}_{\mathrm{a}}^{-1}\left(\boldsymbol{B}_{\mathrm{ua}}\boldsymbol{u}_{\mathrm{a}} + \boldsymbol{f}_{\mathrm{a}}(\boldsymbol{q}, \dot{\boldsymbol{q}})\right)\right)^T \boldsymbol{P}\, \dot{\boldsymbol{e}}_{\mathrm{a}} + \boldsymbol{e}_{\mathrm{a}}^T \boldsymbol{A}\, \dot{\boldsymbol{e}}_{\mathrm{a}} \\ &\quad + \dot{\boldsymbol{e}}_{\mathrm{a}}^T \boldsymbol{P} \left(\boldsymbol{M}_{\mathrm{a}}^{-1}\left(\boldsymbol{B}_{\mathrm{ua}}\boldsymbol{u}_{\mathrm{a}} + \boldsymbol{f}_{\mathrm{a}}(\boldsymbol{q}, \dot{\boldsymbol{q}})\right)\right) + \dot{\boldsymbol{e}}_{\mathrm{a}}^T \boldsymbol{A}\, \boldsymbol{e}_{a}. \end{aligned} \quad (8)$$

The design weighting matrix $\boldsymbol{K}_{\mathrm{Pa}}$ should be satisfied this equality $\boldsymbol{P}\boldsymbol{K}_{\mathrm{Pa}} = \boldsymbol{A}$. Finally, by replacing $\boldsymbol{u}_{\mathrm{a}}$ as a part of the input control $\boldsymbol{u}$ for the actuated joints which are described with subscribe $a$ from Equation (5) to Equation (8) and the weighting matrix constraint, the resulting equation can be formulated as

$$\dot{V} = -\dot{\boldsymbol{e}}_{\mathrm{a}}^T \underbrace{\left(\boldsymbol{P}\boldsymbol{K}_{\mathrm{Da}} + \boldsymbol{K}_{\mathrm{Da}}^T \boldsymbol{P}\right)}_{\boldsymbol{Q}} \dot{\boldsymbol{e}}_{\mathrm{a}}, \quad (9)$$

where $\boldsymbol{Q}$ is a positive-definite matrix and the matrix multiplying condition as $\boldsymbol{B}_{\mathrm{u}}^{-1}\boldsymbol{B}_{\mathrm{u}} = \boldsymbol{B}_{\mathrm{ua}}\boldsymbol{B}_{\mathrm{ua}}^{-1} = \boldsymbol{I}$. Therefore, the derivative of the Lyapunov candidate function is negative-semidefinite. It means that the tracking errors of the active joints are limited. Also, by the limited $\boldsymbol{q}_{\mathrm{a}}$, the passive joints $\boldsymbol{q}_{\mathrm{u}}$ as function of the active joints are limited, too. Hence, the active and passive joints are proofed which are limited. Furthermore, their desired variables are defined as finite time-varying. Furthermore, the tracking errors of the system in Equation (1) under the input controller by Equation (5) are limited and the system is uniformly stable.

For gaining the controlled robot performance and its robustness, the robot feedback controller is supplemented by a disturbance observer to determine disturbances, see Figure 5.

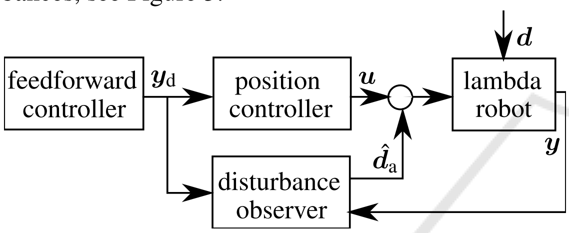


Figure 5: Developed nonlinear feedback control structure under disturbances using a disturbance observer.

The disturbance observer based on its inputs, i.e., desired tracking signals $\boldsymbol{y}_{\mathrm{d}} = [\boldsymbol{q}_{\mathrm{d}}, \dot{\boldsymbol{q}}_{\mathrm{d}}]^T$ and measured signals $\boldsymbol{y} = [\boldsymbol{q}, \dot{\boldsymbol{q}}]^T$, estimates disturbances as $\hat{\boldsymbol{d}}_{\mathrm{a}}$. More details about the design of the disturbance observer is presented in the next part.

## 4.2 Disturbance Observer

The system dynamics reformulation of Equation (4) for the disturbed system is written as

$$\boldsymbol{M}(\boldsymbol{q})\ddot{\boldsymbol{q}} = \boldsymbol{f}(\boldsymbol{q}, \dot{\boldsymbol{q}}) + \boldsymbol{B}_{\mathrm{u}}\boldsymbol{u} + \boldsymbol{d}. \tag{10}$$

In this work, in Equation (12), the disturbance term $\boldsymbol{d} \in \boldsymbol{R}^5$ includes friction forces on the prismatic joints and acted forces on the robot's end-effector. This disturbance term is formulated as

$$\boldsymbol{d} = \boldsymbol{J}\boldsymbol{f}_{\mathrm{ee}} + \boldsymbol{B}_{\mathrm{u}}\boldsymbol{f}_{\mathrm{fri}}, \tag{11}$$

where $\boldsymbol{f}_{\mathrm{ee}}$ being the disturbance forces are acted from the environment to the end-effector, and the Jacobian matrix $\boldsymbol{J}$ for transferring these forces from the workspace to the joint space, and $\boldsymbol{f}_{\mathrm{fri}}$ are the friction forces on the prismatic joints. By projecting the disturbance term as an unknown input for the active joints, the dynamics can be rewritten as

$$\boldsymbol{M}(\boldsymbol{q})\ddot{\boldsymbol{q}} = \boldsymbol{f}(\boldsymbol{q}, \dot{\boldsymbol{q}}) + \boldsymbol{B}_{\mathrm{u}}(\boldsymbol{u} + \boldsymbol{d}_{\mathrm{a}}). \tag{12}$$

The projected term is obtained as $\boldsymbol{d}_{\mathrm{a}} = \boldsymbol{B}_{\mathrm{a}}^{-1}\boldsymbol{J}\boldsymbol{f}_{\mathrm{ee}} + \boldsymbol{B}_{\mathrm{a}}^{-1}\boldsymbol{B}_{\mathrm{u}}\boldsymbol{f}_{\mathrm{fir}}$. By this projection the friction force of the prismatic joints is transferred without change while it is only acted on the actuated joint. In the projection of $\boldsymbol{J}\boldsymbol{f}_{\mathrm{ee}}$, the forces are projected on the active joints and other parts can not be included.

To estimate the disturbance term and to design the input controller for the disturbed system, the disturbance observer approaches in (Chen et al., 2016; Mohammadi et al., 2017; Chen, 2004) are used as a basic idea for the mathematical formulation.

For the disturbed system, the input controller based on the position controller in Equation (5) and the estimation law for the projected disturbance term are formulated as

$$\boldsymbol{u} = \boldsymbol{B}_{\mathrm{u}}^{-1}(-\boldsymbol{f} + \boldsymbol{M}(\boldsymbol{K}_{\mathrm{P}}\boldsymbol{e} + \boldsymbol{K}_{\mathrm{D}}\dot{\boldsymbol{e}})) - \hat{\boldsymbol{d}}_{\mathrm{a}}, \tag{13}$$

$$\dot{\hat{\boldsymbol{d}}}_{\mathrm{a}} = \dot{\boldsymbol{d}}_{\mathrm{a}} + \boldsymbol{H}^{-1}\boldsymbol{M}_{\mathrm{a}}^{-T}\boldsymbol{P}\dot{\boldsymbol{e}}_{\mathrm{a}}, \tag{14}$$

where $\hat{\boldsymbol{d}}_{\mathrm{a}}$ and $\dot{\hat{\boldsymbol{d}}}_{\mathrm{a}}$ are the estimated disturbances and their time derivation. The time derivation of the projected disturbances is presented by $\dot{\boldsymbol{d}}_{\mathrm{a}}$ and the matrix $\boldsymbol{H} \in \boldsymbol{R}^{2\times 2}$ is a positive-definite and invertable matrix. Since there is no information about disturbances on the system, it is assumed that $\boldsymbol{d}$ is a constant or slow varying parameter. Therefore, its time derivation is assumed to be zero, $\dot{\boldsymbol{d}}_{\mathrm{a}} \cong \boldsymbol{0}$, and Equation (14) can be rewritten

$$\dot{\hat{\boldsymbol{d}}}_{\mathrm{a}} \cong -\dot{\boldsymbol{e}}_{\mathrm{d}} = \boldsymbol{H}^{-1}\boldsymbol{M}_{\mathrm{a}}^{-T}\boldsymbol{P}\dot{\boldsymbol{e}}_{\mathrm{a}}. \tag{15}$$

Now, the system stability is investigated for the disturbed situation and it is examined by this new Lyapunov candidate function

$$V(\boldsymbol{e}_{\mathrm{a}}, \dot{\boldsymbol{e}}_{\mathrm{a}}) = \dot{\boldsymbol{e}}_{\mathrm{a}}^T\boldsymbol{P}\dot{\boldsymbol{e}}_{\mathrm{a}} + \boldsymbol{e}_{\mathrm{a}}^T\boldsymbol{A}\boldsymbol{e}_{\mathrm{a}} + \boldsymbol{e}_{\mathrm{d}}^T\boldsymbol{H}\boldsymbol{e}_{\mathrm{d}}, \tag{16}$$

where the projected disturbance estimation error is defined as $\boldsymbol{e}_{\mathrm{d}} = \boldsymbol{d}_{\mathrm{a}} - \hat{\boldsymbol{d}}_{\mathrm{a}}$. For the defined Lyapunov candidate function, its derivative is computed

$$\begin{aligned}\dot{V} &= \left(\boldsymbol{M}_{\mathrm{a}}^{-1}\left(\boldsymbol{B}_{\mathrm{ua}}\boldsymbol{u}_{\mathrm{a}} + \boldsymbol{f}_{\mathrm{a}}(\boldsymbol{q}, \dot{\boldsymbol{q}}) + \boldsymbol{d}_{\mathrm{a}}\right)\right)^T\boldsymbol{P}\dot{\boldsymbol{e}}_{\mathrm{a}} \\ &+ \dot{\boldsymbol{e}}_{\mathrm{a}}^T\boldsymbol{P}\left(\boldsymbol{M}_{\mathrm{a}}^{-1}\left(\boldsymbol{B}_{\mathrm{ua}}\boldsymbol{u}_{\mathrm{a}} + \boldsymbol{f}_{\mathrm{a}}(\boldsymbol{q}, \dot{\boldsymbol{q}}) + \boldsymbol{d}_{\mathrm{a}}\right)\right) \\ &+ \boldsymbol{e}_{\mathrm{a}}^T\boldsymbol{A}\dot{\boldsymbol{e}}_{\mathrm{a}} + \dot{\boldsymbol{e}}_{\mathrm{a}}^T\boldsymbol{A}\boldsymbol{e}_{\mathrm{a}} + \dot{\boldsymbol{e}}_{\mathrm{d}}^T\boldsymbol{H}\boldsymbol{e}_{\mathrm{d}} + \boldsymbol{e}_{\mathrm{d}}^T\boldsymbol{H}\dot{\boldsymbol{e}}_{\mathrm{d}}.\end{aligned} \tag{17}$$

By replacing the actuated part of the $\boldsymbol{u}$ as $\boldsymbol{u}_{\mathrm{a}}$ from Equation (13) and the disturbance estimation law from Equation (15) in (17), the resulting equation can be formulated as

$$\dot{V} = -\dot{\boldsymbol{e}}_{\mathrm{a}}^T\underbrace{\left(\boldsymbol{P}\boldsymbol{K}_{\mathrm{Da}} + \boldsymbol{K}_{\mathrm{Da}}^T\boldsymbol{P}\right)}_{\boldsymbol{Q}}\dot{\boldsymbol{e}}_{\mathrm{a}}. \tag{18}$$

All these conditions for the Lyapunov candidate function and its derivative are fulfilled and, therefore, the system under disturbance $\boldsymbol{d}$ is uniformly stable which explained in the last section. For the nonautonomous case, with Barbalat's lemma in (Khalil, 2002) one can show again convergence of $\dot{\boldsymbol{e}}$ to $\boldsymbol{0}$, but no further statement can be made to convergence of $\boldsymbol{e}$ and $\boldsymbol{e}_{\mathrm{d}}$.

## 5 SIMULATION RESULTS

The goal of the lambda robot controller is to achieve high tracking performance even though disturbing forces are acting on the end-effector or the prismatic joints. To investigate the tracking performance of the designed controllers, i.e., the nonlinear controller and the combination with the disturbance observer from Section 4.2 as (nlc-dob), the nonlinear feedback controller in Section 4.1 as (nlc), and the previously designed feedback linearization controller in (Ansarieshlaghi and Eberhard, 2018b) as (fl), the controlled robot tracks a line trajectory. This line trajectory is time-dependent and starts at point $x_{\text{start}} = [-0.59, -0.5]^T$ and ends at point $x_{\text{end}} = [-0.81, -0.3]^T$ in the robot's workspace. This trajectory shall be followed for 0.5s.

For the lambda robot, the tracking task is implemented on the undisturbed and disturbed system. The disturbances of the lambda robot model are divided into three categories, i.e., disturbances acting on the prismatic joints of the lambda robot, disturbances acting on the end-effector, and the combination of the disturbances acting on the robot joint and the end-effector. The first category includes the friction forces on the robot drivers. The second type of disturbances are forces that are applied to the robot end-effector.

To have a better analysis of the controller's performance, the absolute tracking error of the end-effector (e-abs) and the strain of the long link during tracking time are selected as the benchmarks for the controller's comparison.

As a first task, trajectory tracking of the undisturbed system is simulated. The simulation results of the controllers are shown in Figures 6 and 7. Figure 6 show that the combination of the designed nonlinear controller with disturbance observer has the smallest value of the maximum absolute tracking error. Also, the results show that the maximum value of the absolute tracking error of the controllers is limited in the range of millimeters. The robot's long link desired strain trajectory (d) is compared with the simulation strain of the robot by the controllers.

Furthermore, the zoom view of the strain in Figure 7 at the end part of the trajectory presents that the nonlinear controller combination with the designed disturbance observer converges faster than the nonlinear controller and has smaller oscillation amplitude than the feedback linearization controller.

For the second task, trajectory tracking of the system disturbed by the friction force in the robot prismatic joints is studied. The friction in the prismatic joints is modeled based on the dynamic LuGre model in (Olsson et al., 1998) and the identified parameters of the lambda robot in (Morlock et al., 2015). The simulation results of the system disturbed by friction are depicted in Figures 8 and 9 for the operation as in the first task.

Also, to show the controller's performance at the end of the trajectory tracking, a zoomed view of the long link strain is shown in Figure 9. As shown in Figure 8 and considering the results of the Lyapunov stability of the non-autonomous system, it can only be shown that the tracking error is limited but it can not be proved that it converges to zero.

The third task is defined as the trajectory tracking of the system disturbed by the acting force at the robot's end-effector. This is the second category of the disturbed system. The acting force on the end-effector is formulated in Equation (19) in the global coordinate system of the lambda robot as

$$\boldsymbol{f}_{\text{ee}} = \begin{bmatrix} 1 \\ -1 \end{bmatrix} (0.1 \sin(40\,t) + g(t))N. \tag{19}$$

where $g(t)$ is defined as a scalar in Equation (20)

$$g = \begin{cases} 1, & 0.1s \leq t \leq 0.4s \\ 0, & \text{otherwise.} \end{cases} \tag{20}$$

The acting force on the robot's end-effector is a time-varying function and is composed of the sine and a step function. The simulation results of the disturbed system excited by the applied force in the second category are presented in Figures 10 and 11.

The results show that the designed nonlinear controller combined with the disturbance observer increases the robustness and the performance of the controlled robot. Also, the plotted results of the strain and the absolute tracking error show that the controlled robot compensates the acting disturbances on the end-effector very fast.

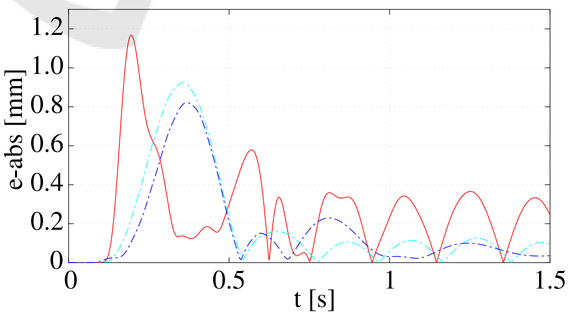


Figure 6: Absolute tracking error for the undisturbed system.

The most complicated and difficult task is the combination of both disturbances categories. Here, the disturbance forces on the end-effector and the prismatic joints are applied to the robot. The simulation results of this task are depicted in Figures 12 and 13.

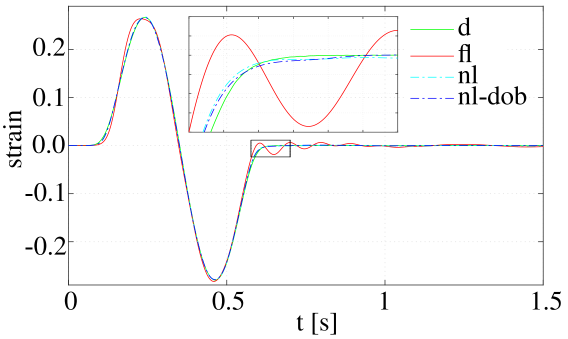


Figure 7: Strain of the long link of the lambda robot model in the undisturbed situation.

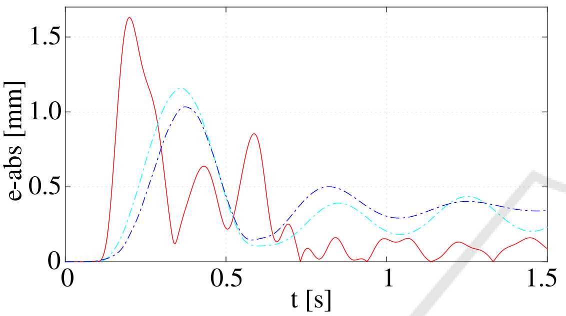


Figure 8: Absolute tracking error for acting friction in the prismatic joints of the robot.

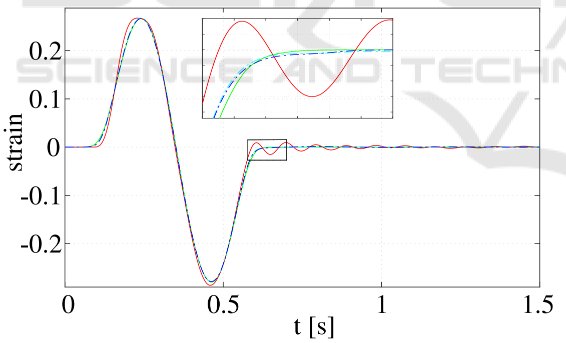


Figure 9: Strain of the long link in the disturbed situation (the prismatic joint's friction).

Figure 12 shows that the absolute tracking error of the robot's end-effector is compensated and the system is adapted to the new situation. Also, the results of the designed controller show high trajectory tracking accuracy. Furthermore, the designed nonlinear feedback controller combination with disturbance observer successfully overcomes the acting disturbances on the robot and the trajectory tracking task is done with high accuracy.

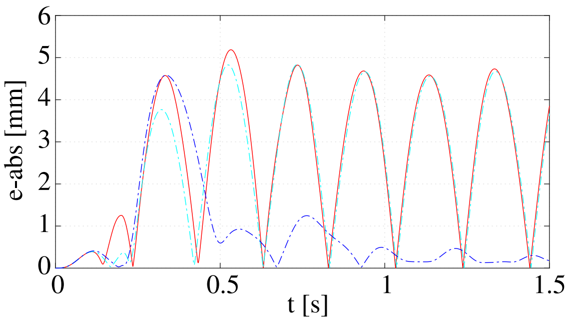


Figure 10: Absolute tracking error in the acting force on the robot's end-effector.

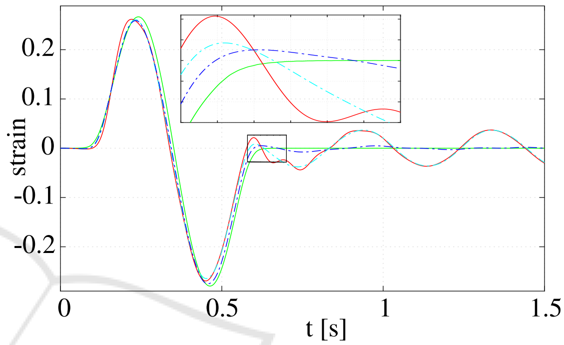


Figure 11: Strain of the long link in the disturbed situation by the force on the end-effector.

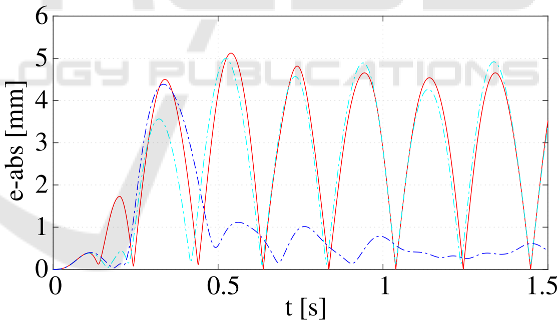


Figure 12: Absolute tracking error of the disturbed lambda robot.

## 6 CONCLUSIONS

In this paper, a high-performance end-effector position controller and its combination with a disturbance observer are presented for a very flexible parallel robot manipulator. The position controller is designed based on the robot model and computes the robot input. To increase the tracking robustness and performance, the nonlinear feedback controller is extended with a disturbance observer in order to estimate the applied disturbances on the system and compensate them.

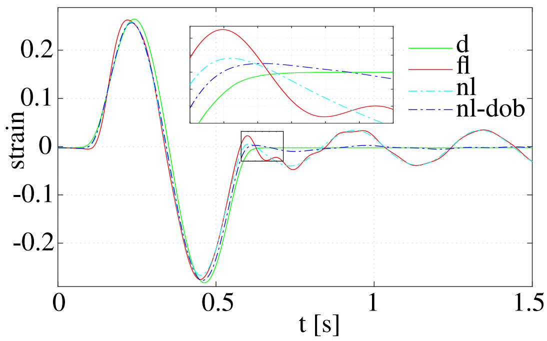


Figure 13: Strain of the long link for the disturbed lambda robot.

The simulation results on the lambda robot model show that the designed nonlinear position controller and combination with disturbance observer based on the flexible model have better performance than other controllers in the trajectory tracking task for the undisturbed system. In the disturbed system, the controller performs very robust and more accurate than other investigated controllers.

For future work, the designed controller will be tested on the real robot and its performance will be investigated. Also, overall disturbances will be applied to the robot model for tracking and interaction tasks.

## ACKNOWLEDGEMENTS

This research was performed within the Cluster of Excellence in Simulation Technology SimTech at the University of Stuttgart and is partially funded by the Landesgraduiertenkolleg Baden-Württemberg.

## REFERENCES

Ansarieshlaghi, F. and Eberhard, P. (2018a). Experimental study on a nonlinear observer application for a very flexible parallel robot. *International Journal of Dynamics and Control*, 7(3):1046–1055.

Ansarieshlaghi, F. and Eberhard, P. (2018b). Trajectory tracking control of a very flexible robot using a feedback linearization controller and a nonlinear observer. In *Proceedings of 22nd CISM IFToMM Symposium on Robot Design, Dynamics and Control*, Rennes, France.

Ansarieshlaghi, F. and Eberhard, P. (2019). Hybrid force/position control of a very flexible parallel robot manipulator in contact with an environment. In *Proceedings of the 16th International Conference on Informatics in Control, Automation and Robotics (ICINCO)*, Prague, Czech Republic.

Burkhardt, M., Seifried, R., and Eberhard, P. (2014). Experimental studies of control concepts for a parallel manipulator with flexible links. In *Proceedings of the 3$^{rd}$ Joint International Conference on Multibody System Dynamics and the 7$^{th}$ Asian Conference on Multibody Dynamics*, Busan, Korea.

Chen, W.-H. (2004). Disturbance observer based control for nonlinear systems. *IEEE/ASME Transactions on Mechatronics*, 9(4):706–710.

Chen, W.-H., Ballance, D. J., Gawthrop, P. J., and O'Reilly, J. (2000). A nonlinear disturbance observer for robotic manipulators. *IEEE Transactions on Industrial Electronics*, 47(4):932–938.

Chen, W.-H., Yang, J., Guo, L., and Li, S. (2016). Disturbance-observer-based control and related methods—-an overview. *IEEE Transactions on Industrial Electronics*, 63(2):1083–1095.

Eberhard, P. and Ansarieshlaghi, F. (2019). Nonlinear position control of a very flexible parallel robot manipulator. In *Proceedings ECCOMAS Thematic Conference on Multibody Dynamics*, Duisburg, Germany.

Han, J. (2009). From PID to active disturbance rejection control. *IEEE Transactions on Industrial Electronics*, 56(3):900–906.

Khalil, H. K. (2002). *Nonlinear Systems*, volume 3. Prentice Hall, Upper Saddle River.

Liu, J., Gao, Y., Su, X., Wack, M., and Wu, L. (2018). Disturbance-observer-based control for air management of PEM fuel cell systems via sliding mode technique. *IEEE Transactions on Control Systems Technology*, 27(3):1129–1138.

Mohammadi, A., Marquez, H. J., and Tavakoli, M. (2017). Nonlinear disturbance observers design and applications to Euler-Lagrange systems. *IEEE Control Systems Magazine*, 37(4):50–72.

Morlock, M., Burkhardt, M., and Seifried, R. (2015). Friction compensation, gain scheduling and curvature control for a flexible parallel kinematics robot. In *Proceedings of the International Conference on Intelligent Robots and Systems (IROS)*, Hamburg, Germany.

Olsson, H., Åström, K. J., Canudas De Wit, C., Gäfvert, M., and Lischinsky, P. (1998). Friction models and friction compensation. *European Journal of Control*, 4(3):176–195.

Seifried, R., Burkhardt, M., and Held, A. (2011). Trajectory control of flexible manipulators using model inversion. In *Proceedings of the ECCOMAS Thematic Conference on Multibody Dynamics*, Brussels, Belgium.